Contemporary Engineering Sciences, Vol. 2, 2009, no. 2, 95 - 104

Performance Prediction of the Single-Sided Linear Induction Motors for Transportation Considers Longitudinal End Effect by Using Analytic Method

Ali Suat Gerçek

University of Gaziantep
Vocational School
gercek@gantep.edu.tr

Vedat M. Karslı

University of Gaziantep
Department of Electrical Engineering
vkarsli@gantep.edu.tr

Abstract

Having the finite length of the stator or rotor of the single-sided linear induction motors (SLIM) leads to negative affect on the performance. These electromagnetic effects occur entry-end and exit- end of the SLIM. The entry end wave reduces the synchronous wave at high frequency operations. An analytic technique based on the equivalent circuit taking into longitudinal end effect and other effects account (transverse edge, saturation etc...) are used to predict the performance of the SLIM. However, in the high speed applications of SLIMs, such as transportation, the performance prediction is very important for design. Analytical tool is developed to predict the performance of the SLIM. This tool is validated with the test results in the literature (Canadian Institute of Guided Ground Transport LIM). The simulation results, which are produced by this analytic tool, are obtained for the designed and constructed SLIM. Results are reported.

Keywords- Linear induction motor, equivalent circuit approach, end effect

1. INTRODUCTION

Single-sided linear induction motor has been applied in the widely used in industrial area. Especially, it is used in transportation. The reason why it is selected the LIM for transportation is the low energy consumption, high speed, and low pollution. Electrical energy converts into mechanical energy and linear motion is achieved. In the design of the LIM, the direct electromagnetic field application is restrictive. Consequently, the equivalent circuit approach is convenient for design and analysis. In the equivalent circuit approach, mutual and secondary parameters are evaluated with the appropriate corrected factor (edge effect, end effect, saturation) for performance prediction. In order to get the high precision result, especially these parameters should be calculated correctly. As further applications for SLIM's are examined, there will be a growing need for analytical tools which will allow the computer-aided design of a machine to a given set of specifications [1-2]-[6].

Several analytical methods that are mainly the direct method, the method of the layers and the method of Fourier series were developed in order to model the linear induction motor. These methods, one by one or combined, made it possible to treat them problems of fields with 1D, 2D and 3D within the linear induction motors [4]. If the air gap flux density is assumed constant, the one dimensional (1-D) analysis method can also be used [8]. In this method, the longitudinal end effect occurs in the air gap as second wave. Consequently, this wave reduces the synchronous wave produced by primary over the high speed range [3]. The problems associated with linear induction motors are relatively difficult to analyze. Several techniques were developed for this end. They can be gathered in two families: analytical methods and numerical methods. All these methods (which are analytical or numerical) start from a formulation of electromagnetic fields resulting from the Maxwell's equations. Those govern all those electromagnetic phenomena, within the electromagnetic devices in a general way and of the linear induction motor in particular.

In this paper, the influences of the longitudinal end effect on the performance of the SLIM with double layer reaction-rail under constant current excitation by using the equivalent circuit are investigated and presented for the designed and constructed SLIM at the different frequency operations by using LIMCAD.

2. END EFFECT EQUATIONS OF THE SLIM

The end effects of a SLIM is due to the finished longitudinal length of the machine and the influence the speed on the nonuniform distribution of the induction of air-gap and the currents induced in the secondary. This effect is taken into account by a correct factor *ke* given on the basis of a distribution of induction in the air-gap of the linear induction motor made up of a field slipping (similar to

the spinning field pattern of the rotary machine) and of an induction being propagated into the direction of the principal field and which is due to the longitudinal effect end [4]:

$$B(x,t) = B_{ms}\sin(\omega t - \frac{\pi}{\tau}x) + B_{me}e^{-\frac{x}{t_e}}\sin(\omega t - \frac{\pi}{\tau_e}x + \delta) \quad (1)$$

The electromotive force induced in a phase of the primary is the superposition of two electromotive forces, one is due to the fundamental field and the other with induction due to the end effect and it can be expressed in the form:

$$e_p(t) = e_s(t) + e_e(t) = -E_{ms}\cos(\omega t) - E_{me}\cos(\omega t) = -E_{ms}(1-ke)\cos(\omega t) \quad (2)$$

Where *ke* is a factor which takes account of the end effect, its expression was established in [4]:

$$ke = -\frac{k_{we}}{k_w}\frac{\frac{\pi}{\tau_e^{\,2}}}{\frac{1}{t_e^{\,2}} + \left(\frac{\pi}{\tau_e}\right)^2} f(\delta)e^{\frac{-p\tau_e}{t_e}}\frac{\sinh\left(\frac{p\tau_e}{t_e}\right)}{p\sinh\left(\frac{\tau_e}{t_e}\right)} \quad (3)$$

Where:

$$f(\delta) = \frac{1}{t_e}\sin\delta + \frac{\pi}{\tau_e}\cos\delta \quad (4)$$

δ is dephasing between the fundamental wave of induction in the air-gap and induction due to the end effect being propagated in the direction of the slipping field, with the entry of the motor. It is approximated in an empirical way by [4]:

$$\delta = \delta_0 + bV_e \quad (5)$$

Where

$$\delta_0 = \pi - \arctan\left(\pi\frac{t_e}{\tau_e}\right)_{V_r=V_0};\ b = \frac{1}{150}\arctan\left(\pi\frac{t_e}{\tau_e}\right)_{V_r=V_0} \quad (6)$$

And

$$V_e = \begin{cases} V_e = \dfrac{V_r - V_0}{V_s - V_0}V_s & if\ \ V_r \geq V_e \\ V_e = 0 & if\ \ V_r < V_e \end{cases} \quad (7)$$

Where V_0 is the boundary speed and it is expressed as,

$$V_0 = 0.5\frac{V_s^{\,2}}{150} \tag{8}$$

τe and *te* represent the pole pitch of the end wave and attenuation factor respectively. It can be calculated by using the following expressions [4]:

$$\tau_e = \frac{2\pi}{D} \tag{9}$$

$$t_e = \frac{2gk_c}{Cgk_c - V_r\mu_0\sigma_{Al}D_{Al}} \tag{10}$$

$$C = \frac{1}{\sqrt{2}}\sqrt{\sqrt{X^4 + 16Y^2} + X^2} \tag{11}$$

$$D = \frac{1}{\sqrt{2}}\sqrt{\sqrt{X^4 + 16Y^2} - X^2} \tag{12}$$

$$X = \frac{\mu_0 V_r \sigma_{Al} d'_R}{k_c\left(g + D_{Al}\right)} \tag{13}$$

$$Y = \frac{\mu_0 \omega \sigma_{Al} d'_R}{k_c\left(g + D_{Al}\right)} \tag{14}$$

Where d'_R. is the thickness of a homogeneous layer out of aluminum equivalent to the two layers which constitute the conducting part of the secondary, it can be used to evaluate resistance modeling the eddy currents in the secondary. This thickness is estimated starting from the equivalent impedance of the secondary. Indeed, the conducting layer out of aluminum and that of ferromagnetic of the secondary are equivalent (from electric point of view) to a layer out of aluminum thickness d'_R, which has as impedance (if it is neglected the effect of skin):

$$Z_{\text{sec}} = (a_R + ja_X)\frac{W}{\tau}k_z\frac{1}{s\sigma_{Al}d'_R} \tag{15}$$

Where $a_R = 1$ and $a_x = 1$ for a nonmagnetic material such as aluminum.

From where d'_R can be expressed the equivalent thickness by identifying the two expressions of (15) and (18).

3. EQUIVALENT CIRCUIT OF SLIM

Equivalent circuit for SLIM is shown in Fig1. Equivalent circuit parameters, which obtained from the electromagnetic 2-D field equations taking into account the saturation , hysteresis , skin, transverse edge, slot effect and the reaction of the eddy current of the secondary , are as follows;

$$z_1^{'} = -\frac{j\omega\mu_0\mu_{re}}{K_1 \tanh\left(K_1 D_{ir}\right)} k_{zv} \tag{16}$$

$$z_2 = \frac{-j\omega\mu_0}{K_2 \tanh\left(K_2 D_{al}\right)} \tag{17}$$

$$z_{\sec}^{'} = \frac{R_{\sec}^{'}}{s} j\frac{X_{\sec}^{'}}{s} = \frac{z_1^{'} z_2}{z_1^{'} + z_2}\frac{1}{s} k_{tr}\frac{L}{\tau} \tag{18}$$

$$z_0 = -jX_M = -\frac{j\omega\mu_0}{\beta \tanh\left(\beta g^{'}\right)} \tag{19}$$

Where $\mu_{re} = \mu\left(\mu^{'} - j\mu^{''}\right)$; $\mu^{'} = a_R a_x$; $\mu^{''} = 0.5\left(a_R^2 - a_x^2\right)$; $k_{tr} = \frac{2m\left(Nk_w\right)^2}{p}$

The saturation factor (k_μ) and equivalent permeability of the back iron (μ_{re}) are calculated using simple iterative method. a_R and a_x depend on the electromagnetic field on the surface of the secondary steel and take account of saturation and hysteresis effect. Saturation effect and slot effect (k_c) modify the air gap length.

$$g^{'} = k_c k_\mu g \tag{20}$$

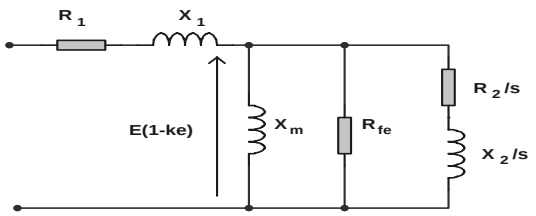

Figure 1. Per Phase Equivalent circuit of LIM

Electromagnetic thrust for the fundamental space harmonic is expressed as

$$F_x = \frac{m(I'_{\text{sec}})^2 R'_{\text{sec}}}{sV_s} \tag{21}$$

Where I'_{sec} is the secondary current referred to primary and expressed as

$$I'_{\text{sec}} = \frac{E_{ms}(1-k_e)}{abs(z'_{\text{sec}})} \tag{22}$$

Symbol definitions are in appendix.

4. SIMULATION RESULTS

Firstly, an analytic tool has been developed for the model of the equivalent circuit and validated with the test result of CIGGT [3] which is shown in Fig.2. Then it was applied to the designed motor using the design parameters presented in Table I and the simulation was carried out.

Table 1
SLIM Data

Parameters	LIM
Motor length,*Lp (mm)*	*1000*
Stack width,*L (mm)*	*250*
Pole pitch, *τ (mm)*	*250*
No. of slot,*z*	*12*
No. of pole,*2p*	*4*
No. of phase,*m*	*3*
Turn per phase,*N*	*80*
Coil pitch,*wc (mm)*	*249*
Air gap length,*g (mm)*	*10*
Secondary width,*W (mm)*	*298.5*
Thickness of conducting plate, *Dal (mm)*	*4.5*
Thickness of the back iron *Dir(mm)*	*20*

All simulation results were obtained at different frequencies (20, 40,60Hz) under constant current excitation (I=100 A) for designed SLIM. The analytic tool was conducted over a range of speed. Thrust as a function of speed at constant current excitation100 A is shown in fig.4. It was calculated for the fundamental space harmonic using the T-type equivalent circuit shown in fig. 1.

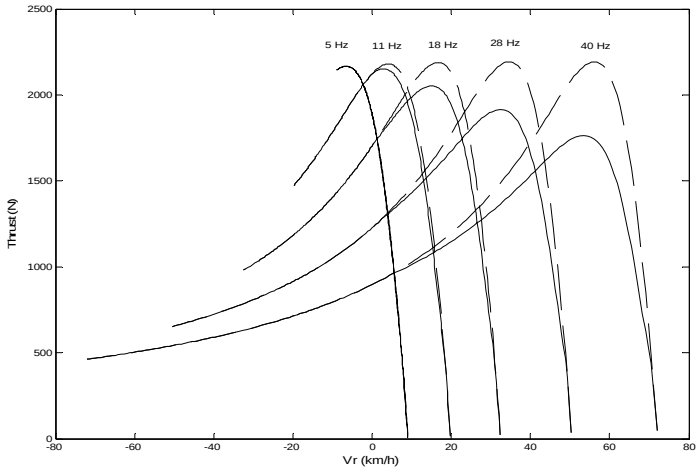

Figure 2 Simulation results of SLIM at different frequency (CIGGT) [6] (broken line- **without end effect**, straight line-**with end effect**)

As expected, the end effect factor increases at high frequency shown in fig.3. This means that the electromotive force (EMF) induced on the primary phase winding decreases. Consequently, the magnetic flux produced by primary decreases. It approaches the negative slope near the synchronous speed for all applied frequencies. And it also shows the variations at low frequencies near the synchronous velocity.

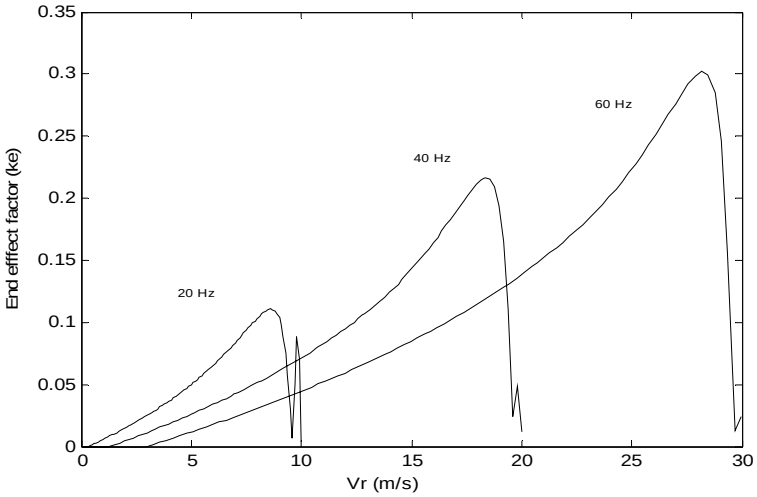

Figure 3 End effect factor at different frequency (20, 40, 60Hz)

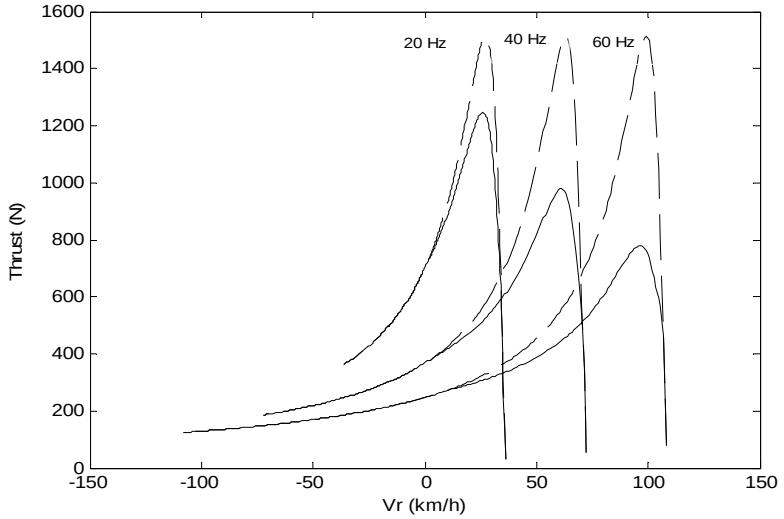

Figure 4 Thrust (broken line- **without end effect**, straight line-**with end effect**)

Under the constant current conditions (I=100A), the maximum available thrust was decreased as the input frequency is increased due to the end effect and influence the saturation of the magnetic circuit and as shown fig.4.

5. CONCLUSION

In this paper, the performance prediction of the designed SLIM using developed analytical tool which agrees with the literature has been performed. Analytical curves in Fig.3-4 have been investigated and evaluated for the performance prediction taking into account end effect. The design consideration agrees with the expected thrust for designed SLIM at 40 Hz. The developed tool may conclude the performance prediction of the SLIM with double layer reaction-rail under constant current excitation over wide range applications.

6. ACKNOWLEDGMENT

All simulations were carried out MATLAB software package release 14. Designed SLIM was constructed in the electric machine laboratory in University of Gaziantep and supported by TUBITAK.

7. APPENDIX

Symbol	Physical Quantity
μ_{re}	*Equivalent permeability of secondary iron*
μ_{rs}	*Surface permeability of secondary iron*
$g_{,}$	*Mechanical clearance*
g	*Effective air gap*
k_{μ}	*Saturation factor*
kc	*Carter coefficient*
Oe	*Slot width*
W	*Secondary iron width*
Lp	*Primary length*
L	*Primary width*
hp	*Height of the primary core*
τ_d	*Slot pitch*
h_e	*Slot height*
l_d	*Tooth width*

REFERENCES

[1] J. F. Gieras, A. R. Eastham and G. E. Dawson, Performance Calculation for Single-Sided Linear Induction Motors With a Solid Steel Reaction Plate Under Constant Current Excitation, In IEE Proceedings, 132, (1985),185-194.

[2] J. F. Gieras,Graham E. Dawson,Anthony R. Eastham, Performance Calculation of the Single Sided Linear Induction Motors wiyh a Double Layer Reaction–Rail Under Constant Current Excitation, IEEE Transactions on Magnetics, 22, (1986).

[3] J. Faiz, H. Jafari, Accurate Modelling of Single-Sided Linear Induction Motor Considers End Effect and Equıvalent Thickness, IEEE Transactions on Magnetic, 36, (2000).

[4] J. F. Gieras, G. E. Dawson and A. R. Eastham, A New Longitudinal End Effect Factor for Linear Induction Motors, IEEE Transactions on Energy Conversion, EC-2., (1987), 152-159.

[5] M. Mirsalim, A. Doroudi,J. S. Moghani, Obtaining the Operating Characteristics of Linear Induction Motor: A New Approach, IEEE Transactions on Magnetics, 38, (2002).

[6] R. M. Pai, Ion Boldea, A Complete Equivalent Circuit of a Linear Induction Motor with Sheet Secondary, IEEE Transactions on Magnetics, 34, (1988).

[7] R. M. Pai, S. A. Nasar and I. Boldea, A Hybrid Method of Analysis of Low-Speed Linear Induction Motors, IEEE Transactions on Magnetics, 23,(1987) 3908-3915.

[8] R. C. Creppe, J. A. C. Ulson, J. F. Rodrigues,Influence of Design Parameters on Linear Induction Motor End Effect, IEEE Transactions on Energy onversion, 3, (2008).

[9] S. Yamamura, , Theory of Linear Induction Motor, Tokyo Press., (1978).

Received: August, 2008